

VIRTUAL COMPONENTS FOR DROPLET CONTROL USING MARANGONI FLOWS: SIZE-SELECTIVE FILTERS, TRAPS, CHANNELS, AND PUMPS

Amar S. Basu*, Seow Yuen Yee, and Yogesh B. Gianchandani
Department of Electrical Engineering and Computer Science
University of Michigan, Ann Arbor, USA

ABSTRACT

This paper describes several microfluidic components, including channels, filters, traps, and pumps, for manipulating aqueous droplets suspended in a film of oil on blank, unpatterned substrates. These “virtual” devices have no physical structure; they accomplish their function entirely by localized Marangoni flows created in a non-contact manner by heat sources suspended just above the liquid surface. Various flow patterns can be engineered through the geometric design of the heat sources on size scales ranging from 10-1,000 μm . Channels and circular traps, emulated by linear and annular heat fluxes respectively, demonstrate nearly 100% selectivity for droplets ranging from 300-1,000 μm . A pump, emulated by a triangular heat flux with a 10° taper, translates droplets of about the same range at speeds up to 200 $\mu\text{m/s}$.

Keywords: Marangoni effect, droplet, filter, channel, pump, microfluidics, thermal probe

I. INTRODUCTION

In droplet-based microfluidic systems, droplet motion is generally guided by microfabricated channels or by interactions with specialized or patterned surfaces. Examples of the latter include electrowetting [1] and dielectrophoresis [2] (both require patterned electrodes), chemical gradients defined during deposition [3], and optoelectronic surfaces [4]. Approaches which do not require specialized substrates include optical tweezers [5]. However, their use in water-in-oil microdroplet systems is made difficult because lasers tend to repel droplets rather than trap them.

This research seeks to eliminate microfabricated features on fluidic substrates. In addition to the evident manufacturing advantages, this can potentially eliminate droplet contact with solid surfaces, reducing the likelihood of sample adsorption to channel walls or other surfaces.

The present approach makes use of the Marangoni effect, *i.e.* the flow on a liquid surface driven by surface tension gradients. Due to the inverse relation between surface tension and temperature, the presence of a temperature gradient on a liquid surface causes Marangoni flow directed from high to low temperature [6]. The small temperature perturbations required to drive Marangoni flow are created by submillimeter-scale heat sources placed just above the surface. The shape of the heat source can be engineered to produce a diversity of flows which can

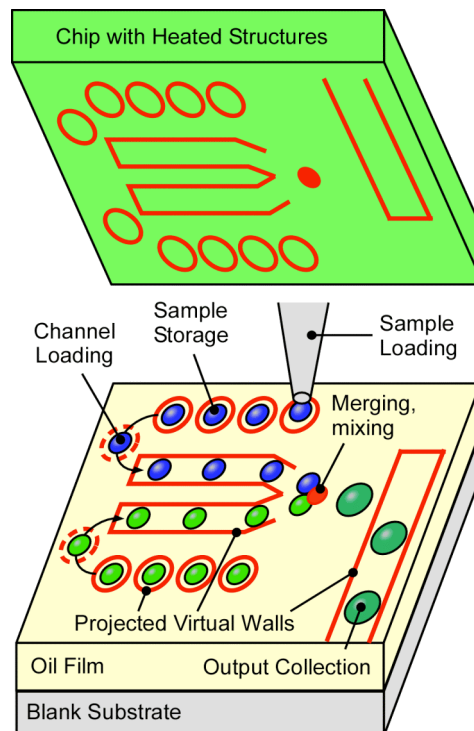


Fig 1: Concept illustration for a microfluidic system driven by suspended heat sources. Various “virtual” fluidic components for droplet manipulation, including channels, filters, traps, and droplet mixers, are all created in a non-contact manner by small temperature perturbations on the liquid surface. On the fluidic substrate, the red lines represent virtual walls formed by Marangoni flows. Only the right-sized droplets are allowed into these virtual structures. Temperature perturbations are created by a separate structure suspended above the substrate.

emulate integral microfluidic components such as channels, traps, and pumps. Together, these virtual components are building blocks toward a microsystem for droplet-based assays (Fig. 1). In addition to reducing the complexity of the substrate, another advantage of this approach is that it does not require the actuators to contact the liquid; thus, the actuators can be reused without contamination concerns. Initial simulations also suggest that Marangoni actuation can achieve >1 mm/s flow velocities with changes in surface temperature on the order of 1°C or even less.

Our past work [7-8] focused on the most basic heat source geometry: a point source. This pattern generates an axisymmetric toroidal flow cell directed outward on the surface, and inward below the surface. Flow velocities up to 1.7 mm/s were achieved in several mineral oils with <20 mW power, and the recirculating flows were used to hold,

* Address: 1301 Beal Avenue, Ann Arbor MI 48109-2122, USA; Tel: (734) 647-2040; Fax: (734) 647-1781; Email: basua@umich.edu

merge, and pre-concentrate aqueous droplets suspended in the oil. This effort reports more complex droplet operations that can be achieved by further engineering the geometry of the heat flux, and by taking advantage of Marangoni flows at both surface and subsurface levels. Size-selective droplet channels, droplet traps, and pumping are systematically designed and demonstrated. Each component is discussed in turn.

II. SIZE-SELECTIVE VIRTUAL CHANNELS AND TRAPS

Size-selective channels collect droplets within a specific range and confine them within its boundaries (Fig. 2). They are formed by parallel heat sources separated by a spacing s . When placed above a layer of oil, the sources project two linear heat fluxes on the liquid surface which define the virtual walls of the channel (Fig. 2a). The range of droplets captured within the channel is a function of the spacing s . Target-sized droplets are pulled into the channel; others are pushed out.

The parallel heat sources create two local peaks in surface temperature. The resulting Marangoni flow is comprised of two recirculating cells on opposite sides of the heat sources, and a relatively still region between them (Fig. 2b). Surface flows are directed away from the channel, and subsurface flows are directed toward it. Droplets of appropriate size are pushed into the channel by the subsurface flows, which apply a lateral force to the center of mass of the droplet. The surface flows, which apply only a tangential force on the top side of the droplet, do not cause lateral movement. They do, however, affect smaller droplets, whose center of mass is closer to the surface. These droplets become trapped in the recirculating flows and are therefore excluded from the channel. The distinction between ‘large’ and ‘small’ droplets is a function of s .

A second, equally viable way to create a virtual channel (not illustrated) is with a single line heat source instead of two parallel sources. In this case, the channel size and the droplet size-selectivity are defined by the width of the heat source (w) rather than the spacing s . The double line heat

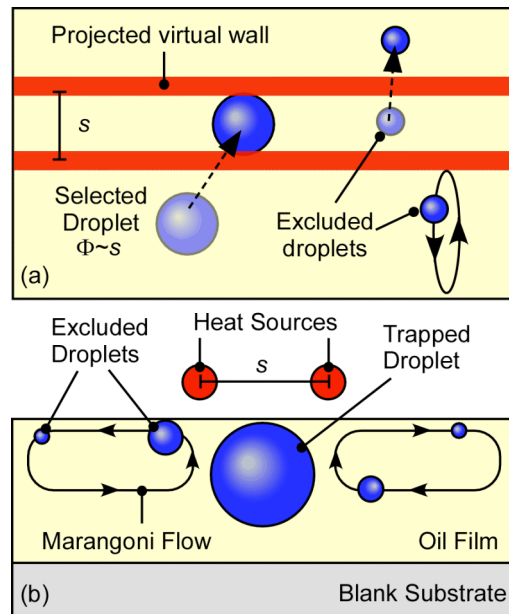


Fig 2: Virtual droplet channels. (a) Virtual channel projected by two heated wires with separation s held parallel to the liquid surface. Target-sized droplets are pulled into the channel; others are excluded. (b) Cross section schematic illustrating principle of operation. Recirculating flows occurring as a result of the Marangoni effect are shown with arrows. The large droplet is trapped in the virtual channel region.

source offers some flexibility in that virtual channel region be easily made much wider than the single line channel.

Both techniques can be simulated using a computational fluid dynamics (CFD) solver (FLUENT 6.0, Fluent Corp). The appropriate surface heat flux is placed as a boundary condition on a 3-dimensional fluid layer, the bottom of which is held at ambient temperature. The simulator calculates the Marangoni flows using an iterative procedure which includes the following steps: 1) calculating the surface temperature profile gradient using a heat conduction simulation, 2) equating the surface temperature gradient to surface shear stresses, and 3) solving the constituent fluid flow equations with the shear stress as a boundary condition.

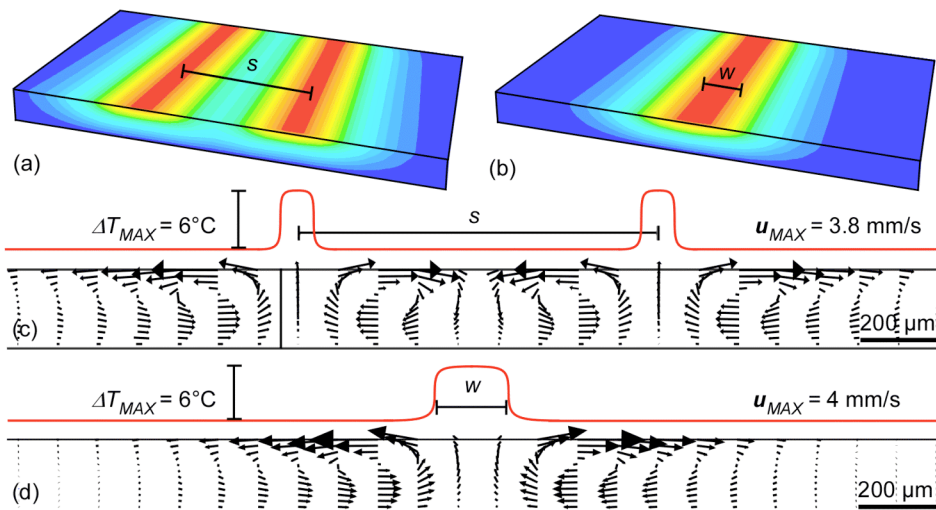


Fig 3: CFD simulations of virtual droplet channels. (a,b) Surface and cross section temperature profiles resulting from (a) 2 parallel linear heat sources with a spacing $s=900 \mu\text{m}$, and (b) a single line heat source with width $w=350 \mu\text{m}$. (c,d) Flow vectors resulting from (c) the parallel heat sources, and (d) the single line heat source. In each case, surface temperature profiles are drawn above the flow vectors. Simulations assume a $200 \mu\text{m}$ -thick mineral oil layer with a surface tension coefficient $-0.16 \text{ mN/m}\cdot\text{K}$. Heat flux amplitudes are $6,000 \text{ W/m}^2$. u_{MAX} is the maximum flow velocity, and ΔT_{MAX} is the max surface temperature change.

Simulation results (Fig. 3) illustrate the differences in flow patterns of the double and single line heat sources. Recirculating flows are present inside the double line channel but do not appear in the single line version. Experimentally, these internal flows do not appear to affect the trapping capability of the channel. It is notable that in both cases, up to 4 mm/s surface velocities can be obtained with $<6^{\circ}\text{C}$ change in surface temperature. This illustrates the favorable scaling of Marangoni flows: surface effects tend to dominate in thin fluid layers, which allows Marangoni flows to be an efficient micro-scale actuation technique. The subsurface flows are only about 1/3rd the velocity of the surface flows, but they are sufficient to pull in selected droplets.

The functionality and size-selectivity of droplet channels were experimentally verified by placing two parallel, cylindrical metal structures above a thin layer of phenylmethyl polysiloxane oil (PMPS, Dow Corning 550 Fluid). This particular oil was chosen for its high density (specific gravity=1.07), which causes the aqueous droplets to float on the oil surface. Droplets with diameters ranging from 20-2,000 μm were pipetted into the oil. Larger droplets tended to adopt a pancake shape rather than a perfect sphere due to the buoyant force against the oil surface. The metal structures were heated to approximately 110°C with an attached soldering iron and placed 200 μm above the oil surface. Droplets within a specific size range move into the channel, and smaller droplets are actively removed from the channel by the Marangoni flows (Fig. 4a). Very large droplets are unaffected by the flows, and therefore are not actively recruited into the channel.

The ability to tailor the size selectivity of the channels is quantitatively shown in Fig. 4b. A histogram of droplet

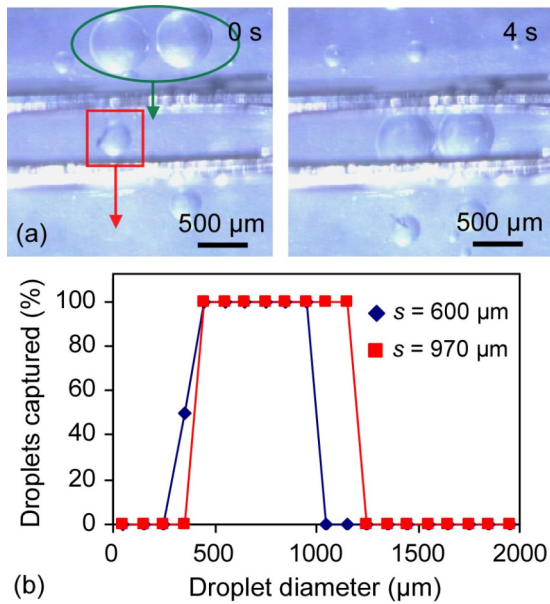


Fig 4: Droplet filtration capability of virtual channels. (a) Micrographs showing two $\phi=500 \mu\text{m}$ droplets (circle) entering the channel while a smaller one (square) is rejected. (b) Histogram showing the size selectivity of two droplet channels with 600 μm and 970 μm spacing. Droplet statistics were compiled over video clips spanning 40 minutes. Bins are in 100 μm increments.

capture vs. droplet size is shown for two channels with different spacings (s). When $s=600 \mu\text{m}$, the minimum diameter for entry into the channel is 250 μm , and when $s=970 \mu\text{m}$, the minimum diameter is 350 μm . A sharp transition can be seen in both cases, and nearly 100% exclusion of off-sized droplets is shown. Therefore, these channels inherently provide an effective size-based filtration capability.

The single droplet trap is implemented using a ring-shaped annular heat source (Fig. 5). The primary difference between this component and the channel is that the droplet is confined in both lateral dimensions. The trap is useful as a reservoir for holding single droplets, and for manipulating droplets if the heat source is translated laterally. The simulated flow vectors along a cross section of the ring are identical to those shown in Fig. 3c; however, when viewed from above, the flow pattern is axially-symmetric about the heat source. The subsurface flows (Fig. 5b), composed of two distinct regions, are responsible for droplet trapping. Flows along the perimeter of the ring, oriented inward, push

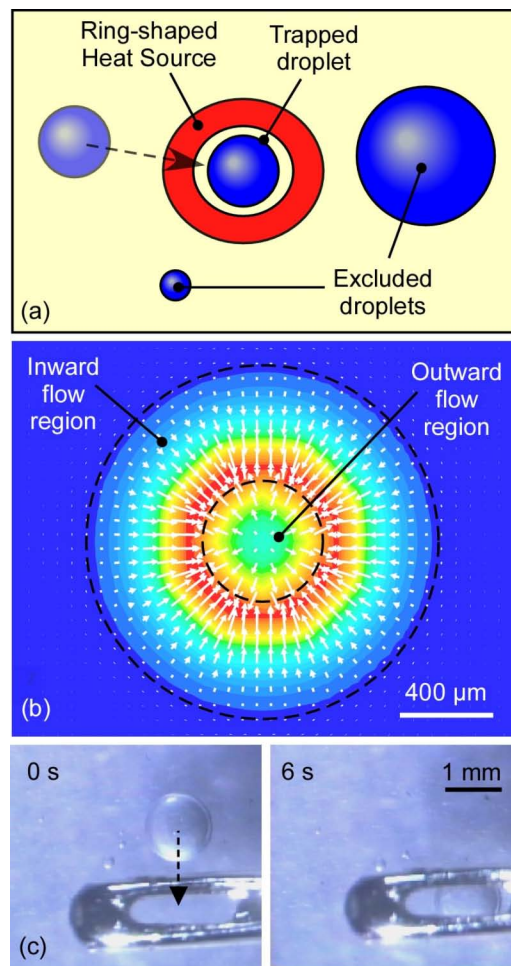


Fig 5: Single droplet trapping with an annular heat flux. (a) Schematic illustrating a trapped droplet and the exclusion of larger or smaller droplets. (b) CFD Simulation. The shaded contours represent the surface temperature gradient. White arrows represent the subsurface flow (140 μm depth). The two regions of flow are marked with dashed lines. (c) Micrographs showing affinity of a droplet to the annular heat source ($T \approx 120^{\circ}\text{C}$). Gap is $\approx 200 \mu\text{m}$.

the droplet to the center. Within the boundaries of the ring, the flow vectors are oriented outward, but these flows do not affect the trapped droplet because the body forces they impart on the droplet are symmetric and therefore cancel each other. The surface flows (not shown), which are always oriented opposite the subsurface flows, reject smaller droplets from the trap. Therefore, the size exclusion capability applies to this geometry as well.

Figure 5c shows experimental results. A rectangular ring-shaped metal pin ($T \approx 120^\circ\text{C}$, $s = 600 \mu\text{m}$) is suspended $\approx 200 \mu\text{m}$ above a PMPS oil layer to approximate an annular heat flux. Figure 5 shows that a $\phi = 700 \mu\text{m}$ droplet is actively pulled into the trap, driven by the subsurface flows directed into the channel. If the trap boundary is moved (by the translation of the substrate or heat source), the droplet follows it. Droplet velocities are $\approx 200 \mu\text{m/s}$.

III. GUIDEWIRE PUMP

Pumping or actuation of droplets can be accomplished by two methods. The first is simply a consequence of the trapping: the heat source projecting a channel or a trap can be translated physically with respect to the substrate, and the trapped droplets follow it. However, droplet actuation can be also accomplished by steady-state, motionless heating provided by a tapered shape and angled spacing (Fig. 6). This geometry provides a triangular heat flux on the fluid surface, and a temperature gradient oriented in the direction of increasing width. The resulting subsurface flows (Fig. 6b) are biased in the direction of increasing taper, and can push appropriately sized droplets along the length of the guidewire. The surface flows (not shown) are biased in the opposite direction, and they reject small droplets from the guidewire similar to the previous components.

Figure 6c shows a guidewire pump projected by a steel needle ($T \approx 130^\circ\text{C}$) with 10° lateral taper, and a 5° taper in vertical spacing. The $\phi = 523 \mu\text{m}$ droplet is pulled from left to right by virtue of the Marangoni flows. The droplet achieves a maximum velocity of $196 \mu\text{m/sec}$.

CONCLUSIONS

Several components for droplet manipulation were presented, all of which operate without physical structures solely by localized Marangoni flows. The distinguishing aspects of this approach are that 1) it is a non-contact method of actuation, 2) droplets do not make contact with solid surfaces, 3) it does not require patterned substrates, and 4) a size-filtration capability is inherent to each component. The favorable scaling of surface forces also makes Marangoni actuation a promising approach to microfluidics. Future work will be directed at combining the various components to create a functional system for microdroplet-based assays.

ACKNOWLEDGEMENTS

Partial support for this effort was provided by the NSF, NIH, the University of Michigan, and a Whitaker Foundation Fellowship (AB).

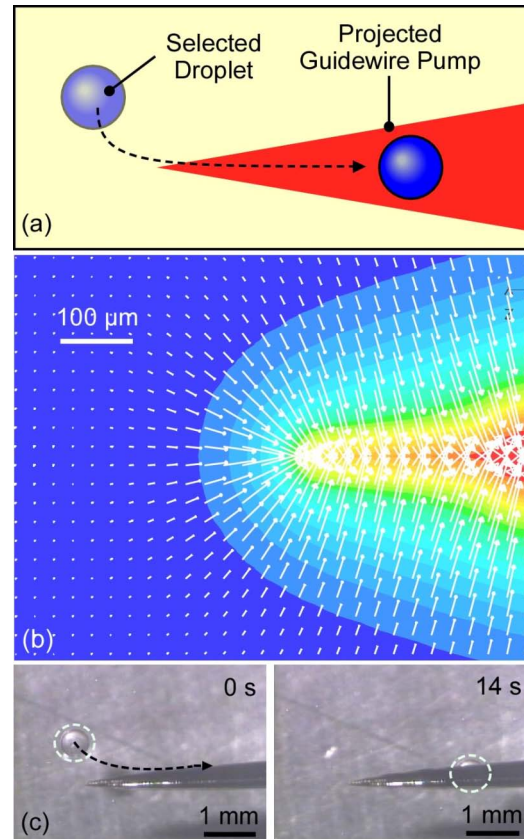


Fig 6: Guidewire pump. (a) A triangular heat flux projected on the fluid surface pulls droplets in and along its longitudinal axis. (b) CFD Simulation. Shaded contours represent the surface temperature gradient, and white arrows represent the subsurface flow ($140 \mu\text{m}$ depth) which pushes a droplet from left to right. (c) Micrographs illustrating movement of droplet at $196 \mu\text{m/s}$ caused by a suspended heat source ($T \approx 130^\circ\text{C}$) with 10° lateral taper and a 5° taper in vertical spacing. Gap is $\approx 200 \mu\text{m}$.

REFERENCES

- [1] S.K. Cho, H. Moon, C.-J. Kim, "Creating, transporting, cutting, and merging liquid droplets by electrowetting-based actuation for digital microfluidic circuits," *J. Microelectromech. Sys.*, vol. 12, pp. 70-80, Feb. 2003.
- [2] T.B. Jones, M. Gunji, M. Washizu, M.J. Feldman, "Dielectrophoretic liquid actuation and nanodroplet formation," *J. Appl. Phys.*, vol. 89, pp. 1441-1448, Jan. 2001.
- [3] M.K. Chaudhury, G.M. Whitesides, "How to make water run uphill," *Science*, vol. 256, pp. 1539-1541, June 1992.
- [4] P.Y. Chiou, Z. Chang, M. Wu, "Light Actuated Microfluidic Devices," *Proc. MEMS*, 2003, pp. 355-358
- [5] A. Ashkin, "Application of radiation pressure," *Science*, vol. 210, pp. 1081-1087, Dec. 1980.
- [6] F.J. Higuera, "Steady thermocapillary-buoyant flow in an unbounded liquid layer heated nonuniformly from above," *Phys. Fluids*, vol. 12, pp. 2186-2197, Sept. 2000.
- [7] A.S. Basu, Y.B. Gianchandani, "Trapping and Manipulation of Particles and Droplets Using Micro-Toroidal Convection Currents," *Proc. Transducers*, 2005, pp. 85-88.
- [8] A.S. Basu, Y.B. Gianchandani, "Microthermal Techniques for Mixing, Concentration, and Harvesting DNA and Other Microdroplet Suspensions," *Proc. μTAS* , 2005, pp. 131-134.